Original Research Article

aeroacoustics

Playing flute without lips? Tones of music lost in time:An investigation of the indigenous Bastar flutes of India

International Journal of Aeroacoustics
2023, Vol. 0(0) 1–21

DOI: 10.1177/1475472X221150176
journals.sagepub.com/home/jae
SAGE

Ashish Karn, Ritvik Anand, Aditya Kataria, Ramesh Kumar Donga, Naman Agarwal and Varun Pratap Singh

Abstract

The physics of music has been well studied and has provided the basis on which musical instruments are made, studied and characterized. Significant research has been conducted on the different kinds of musical instruments, which range from traditional instruments like the *mridangas* of India to the bagpipes of Scotland. In fact, a lot of research has been carried on the acoustics of different kinds of flutes as well, such as the Finnish kantele and the Indonesian Kompangs. The Indian subcontinent, the birthplace of transverse flutes and a host of other instruments, itself has a plethora of unique musical instruments that have been scientifically examined. Yet, the Bastar flutes of India have evaded the due scientific attention that they deserve owing to their unique sound generation mechanism. Quite strangely and surprisingly, these Bastar flutes are a unique genre of flutes that don't require lips to be played, and are quite intriguing. The current research explores the aeroacoustics of a Bastar flute via experimental measurements, computational simulations and analytical formulations. The results demonstrate that the amplitude produced is directly proportional to the number of rims present. This are also responsible for producing a low-frequency, high-amplitude melodious sound. It also suggests that the underlying mechanism behind sound generation in a Bastar flute is a unique blend of edge tone and a jet tone, demonstrating a rare phenomenon not seen in traditional musical instruments. This uncommon phenomenon has the potential to unlock several new applications in the field of acoustics.

Keywords

Aeroacoustics, Bastar flute, centrifugal force, fluid dynamics

Date received: 10 May 2022; revised: 17 December 2022; accepted: 21 November 2022

MultiPhase Flows Laboratory, Department of Mechanical Engineering, School of Engineering, University of Petroleum and Energy Studies, Dehradun, India

Corresponding author:
Ashish Karn, Department of Mechanical Engineering, School of Engineering, University of Petroleum and Energy Studies, Energy Acres, Bidholi, Dehradun 248007, India.
Email: akarn@ddn.upes.ac.in

Introduction

A Gond tribal walks through the forest, apparently holding a bamboo in his hand, gently fiddling and rotating the bamboo that produces a mellifluous music, charming the animals and humans alike. What looks like a plain bamboo stick, as shown in Figure 1, produces melodious tones that have been used traditionally by these communities since time immemorial for hunting and recreation alike. At the first instance, however, it is a shocking revelation to a layman that a mere rotation of a hollow stick should produce such amazing tones. Indeed, the reductionist approach behind understanding sound generation mechanisms entails viewing sound as simply the pressure variations in the air molecules that are sensed by the ears of an organism. Yet, the tones are intriguingly pleasant to human ears!

Indeed, humans have been using these sounds to their advantage for a long time in activities like hunting, communicating, and music. Recent studies have even shown that not only humans but animals also use sounds to interact with humans. Chimpanzees use special sounds to attract human attention when kept in enclosures[1] and the sounds produced by birds help to relax humans.[2] Also, there are many ways in which humans have developed the use of sound in new application areas for interactive sound, beyond the domains of speech and music. These range from teleoperation and way-finding, to peripheral process monitoring and augmented environments.[3] Over time, humans have created various instruments that facilitate their daily activities. Multiple studies have reported a lot of instruments to analyze their sound characteristics and have employed the role of vortices as the primary producer of sound and used various models to explain its presence.

Musical instruments are generally distinguished into five different types: strings, woodwind, brass, keyboards, and percussion.[4] The focus of this study will largely be on the woodwind instruments, the flutes in particular. Many other Indian instruments, both stringed and percussion based, have been analyzed to understand how they produce sound, most notably by C.V. Raman, an Indian noble prize winning scientist.[5–7] The experimental approach to understanding these instruments have led to the discovery of various phenomena. These phenomena are critical in building scientific models that are applied to understand the general theories of sound.

Figure 1. The Bastar Flute. Notice the engravings and carvings on the flute surface depicting human figures, and other nature-inspired patterns.

Flutes have been categorized into seven types: Piccolo flute, Alto flute, Bass flute, Wooden flute, Eb Soprano flute, Concert flute and Plastic flute.[8] Cultures around the world have had variations of these seven flutes which have piqued the interest of researchers and musicians alike. A plethora of studies have been done on these traditional flutes and other instruments like the Finnish Kantele,[9] the Kompang,[10] the Indonesian Gamelan,[11] the Irish flute[12] and the Japanese Bamboo flute[13] to name a few. Although flutes are the oldest musical instrument used by humanity, as evidenced by references of flutes in the ancient Hindu text *Rigveda*,[14–16] the Indian classical flute has received very less academic attention till date.[17]

The *Bansuri*, the bamboo flute (Indian classical flute) is a side-blown instrument with its roots in India. The air blown is responsible for the oscillation of the air column in the flute passage and produces a variety of sounds depending on the volume of the exit. As a consequence of this, the various notes are arranged in the form of an octave, and at the moment there are two octaves in practice. By blowing over the blowhole (or embouchure hole), the flute becomes a resonator and produces sound. When the air jet hits the edge of the blowhole at an angle, called the blow angle, the tube's oscillations speed up. As a result of a column of air within the flute vibrating, sound is emitted from the instrument.[18] A bamboo flute used in Hindustani classical music has anywhere from six to seven holes spaced evenly throughout its length. One end of the tube is sealed off by the embouchure hole while the other is exposed to air. This type of flute can generate two octaves, or two and a half octaves in the hands of a skilled musician. Separating the frequencies heard before and after the hole is opened is crucial. These estimates become quite simple and accurate when the location of each hole in question is known with absolute certainty. Due to the nature of the excitation mechanism instrument in flute, a range of embouchure hole coverage is required. By increasing this covering at the embouchure hole, the note becomes flatter, and the impact created by articulation of sound inside the bore is reduced. The lower the frequency, the longer the wavelength of the note, and the higher the frequency, the shorter the wavelength of the note (higher octave). In general, the relationship between frequency and wavelength is proportional. For a high-pitched note, the player must over-blower and increase the air pressure at the embouchure hole, thereby moving the octave up a level. Displacement nodes and pressure nodes are created inside the tube. Pressure at the tube's open end is inversely proportionate to that at the other node, and air pressure dominates at both. Blown at speeds anywhere from 20 to 40 m/s,[19–21] the pressure within the flute is somewhat greater (∼1 kPa) than ambient pressure. The spectra fluctuate very little from note to note, and these changes have little to do with vowel articulation or timbre (which is altered by different finger placements over the sound hole).[22] Variations on an artificially blown and mechanically agitated flute head joint are used to compute the complicated acoustic back pressure created by the blowing jet. The ratio of the lip aperture area to the tube cross-section area is used to determine the acoustic back pressure intensity, which in turn is derived from the jet momentum as being roughly double the static blowing pressure. The period of the generated backpressure with respect to the oscillation volume velocity is based on the lip-to-edge distance and the velocity of propagation of a wave on the jet. The adjustment made during this time interval is demonstrated to be the major means by which the flutist chooses the desired mode of oscillation of the instrument. Low efficiency (∼2.4%) of jet power conversion to acoustic oscillation power in decibels-milliwatts (approximately equivalent to the ratio of particle velocities in the air column and the jet) is seen at 440 Hz.[23]

Although the earliest form of transverse flute originated in India,[24] there are not many flutes even in India that can be played without lips. One of such flutes commonly reported in the literature is the nasal or nose-flute of Bengal that has been depicted in the etchings of Solvyns[25] (sec XI, No. 36) . However, another flute of such kind that has not been reported is the Bastar flute, that produces sound by the rotation with a hand, and has been used by the Maria and Muria, the Gond tribes in

Chhattisgarh, India for hunting and ceremonial purposes.[26,27] The flute mechanism is quite simple as the main body consists of a long hollow bamboo stick with two to three thin metal rings on one end. It can be observed that to produce sound, the stick needs to be rotated around a fixed point in a centrifugal motion with the end with the rings being on the outer side. As the flute rotates, the compression of the air, which is the working fluid, takes place. As this kind of experimentation and validation has never been done before, this paper aims to find an explanation behind the generation mechanism of the sound, as well as its characterization.

Of course, a number of theories and models have been proposed till date on the mechanism of sound generation per se. Yoshikawa et al. in 2012 noted that the model of jet vortex-layer development is more applicable to sound generation than the vortex-shedding model.[28] The fluctuating Coriolis force induced by the interplay of potential and vertical fluxes is shown to be the sole component in the linearized momentum equation that is not immediately balanced by a fluctuating pressure gradient by Nelson et al.[29,30] Howe[31] established the foundation for a novel acoustic analog, and the related acoustic source terms are only connected with portions of the flow where the vorticity vector and entropy-gradient vector are non-vanishing. In the presence of a low, subsonic mean flow of uniform mean density, he also discovered a general formula for the rate at which acoustic energy is wasted at the sharp edges of a rigid barrier by the creation of vorticity.[32] Salikuddin observed that in all test circumstances, including no flow, a low-frequency acoustic power loss phenomenon was seen for all designs. The power loss seen in the absence of flow was thought to be caused by the conversion of acoustic energy into vertical energy due to the non-linear propagation of high-intensity pulses.[33] Multiple studies also use flow visualization techniques like PIV,[34–36] while some studies use computational methods to understand the sound produced.[37,38]

To understand the sound produced by the "Bastar flute", some experimental investigations and computational simulations has been conducted in the present study to understand the underlying process. The current paper has been structured as follows: The next section describes the experimental setup used and the methodology used to conduct the experiment. Next, the results of the experiment along the various axis, the mathematical modelling of these results and the comparison between the flutes of different rims. Finally, the paper concludes with an understanding of the methods used and discusses gaps and further research that can be conducted.

Material and methods

Experimental setup

The experimental setup comprises of a computer with MATLAB software installed for data acquisition and signal processing, a wired microphone to record the signal, and a Bastar flute, that covers the physical variable of the acoustic study. The microphone used in the experiment is a BOYA omnidirectional microphone with a frequency range between 65 Hz $\sim$ 18 KHz and has a built-in condenser. The mode of transmission is wired. The microphone is attached to the flute with the help of a simple tape. The inner part of the flute consists of rims located at one end of the flute and the rest is hollow till the other end, the microphone is attached to the upper end as shown in Figure 2. In addition, a camera with slow-motion imaging features and a light source were used for filming the flute rotation to compute the angular velocity. A Nikon DSLR camera (Model D7500) was used for imaging purposes and it can capture the videos at a maximum of 60 frames per second.

The length of the flute is 820 mm and the outer diameter of the material is 30 mm. There is a rim present inside the flute which has an outer diameter of 24 mm and an inner hollow diameter of 10 mm. There are 2 rims placed consecutively next to each other at a distance of 3.5 mm. The

Figure 2. Arrangement of the microphone on top of the flute.

thickness of each rim is 0.5 mm. The dimensions of the flute are shown in Figure 3. Table 1 further enlists the specifications of all the components.

Experimental methodology

Sound is generated in the flute when it is rotated at a certain RPM about any X and Y when the rotation is imparted manually as shown in Figure 4. In all the performed experiments, the rotation is done by keeping the rim at the free end. The RPM in all the experiments was maintained at an approximately constant 100 RPM (varies within ±5%), which is confirmed by the high-speed video taken from the experiments.

It is imperative that the microphone not be disturbed by any vibrations or movement, hence special care is taken to achieve this. Changes in the SPL spectrum would be an unwanted side effect of such unwanted motion. Our ability to reproduce results at each setting is evidence that such vibrations are not present in our experiments. There was negligible background noise in our experiments, and background removal was also performed on the raw recorded data. As the rotation is imparted, post-processing is also done simultaneously with it and hence the FFT is produced instantaneously. Hence, the time of rotation can depend on the limit set in the signal processing; hence in our case, a time limit of 5 seconds is considered; after this, the signal processing would cease immediately. To ensure that the experiment is properly performed, a set of cumulative experiments is performed to correlate with the previous data, and further experimentation is carried out.

The post processing is done on MATLAB, which gives the Fast Fourier Transform (FFT) of the signal, giving us three parameters at a time, i.e., amplitude, frequency, and spectrogram. The schematic of the experimental setup is shown in Figure 5 and the experimental setup is shown in Figure 6. Figure 7 presents a flowchart outlining the experimental methodology. As the figure shows, before conducting the experiments, an ambient check is done to measure the background noise and ensure that there is no interference with the measured physical variable. Therefore, all the

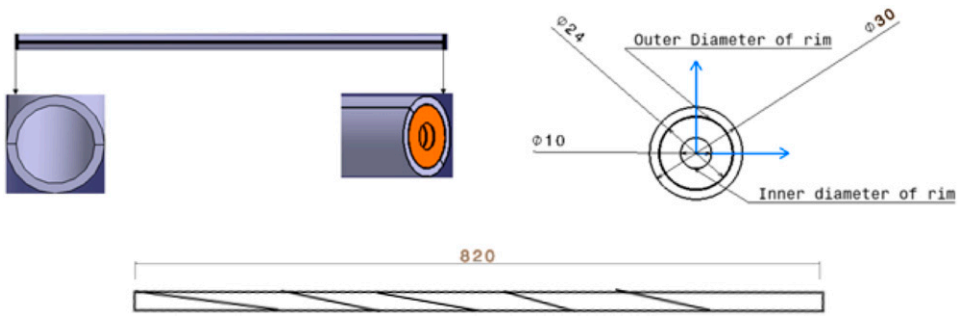

Figure 3. Dimensions of the flute (All dimensions are in mm).

Table 1. List of Components with their specifications.

S.N.	Component	Description
1.	Flute	1. Total length – 820 mm 2. Outer diameter – 30 mm 3. Inner diameter – 24 mm 4. Material - Bamboo
2.	Rim	1. Outer diameter – 24 mm 2. Inner diameter – 10 mm 3. Thickness – 0.5 mm 4. Distance between two consecutive rims – 3.5 mm
3.	Microphone	1. Signal direction – Omnidirectional 2. Frequency range – 65 Hz ~ 18 KHz 3. Built-in condenser 4. Wired transmission

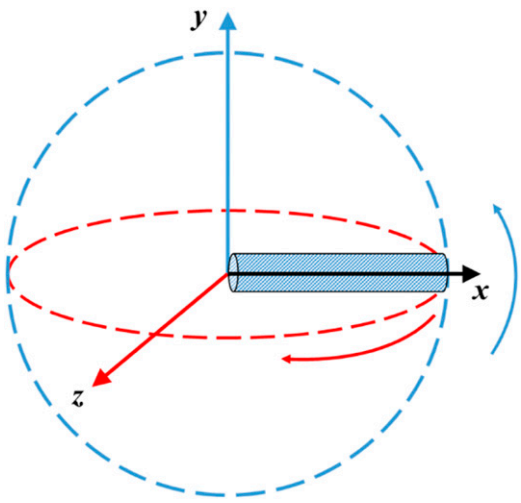

Figure 4. Flute rotational axes.

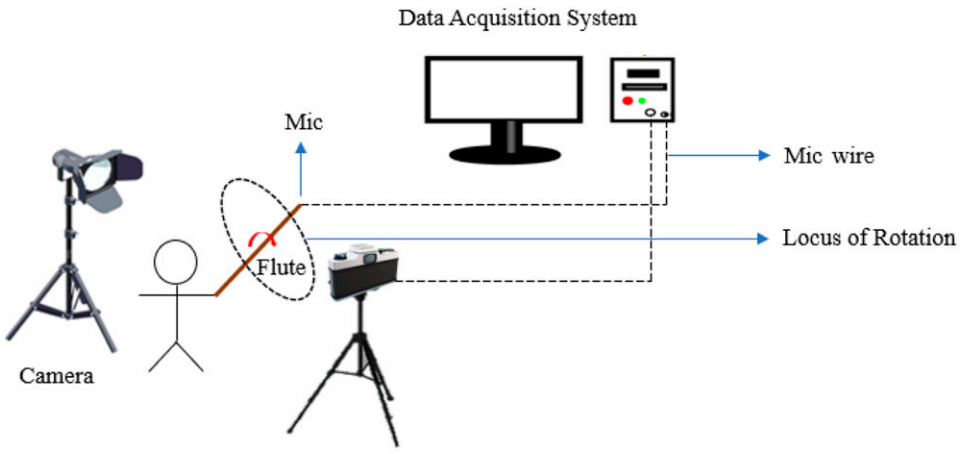

Figure 5. Schematic of the experimental setup.

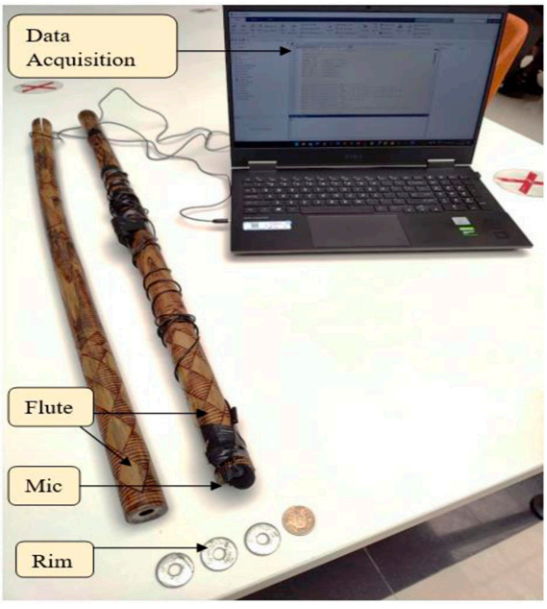

Figure 6. A picture of the experimental setup.

experiments produced in the results section are done in an almost quiet environment, as recorded by the unidirectional microphone. In sync with the post-processing, the camera records the entire experiment for the calculation of RPM and further analysis.

Simulation methodology

Simulations are performed using finite volume method on structured mesh. ICEM CFD software is used to generate mesh. The Fluent software has been used to perform the simulations for

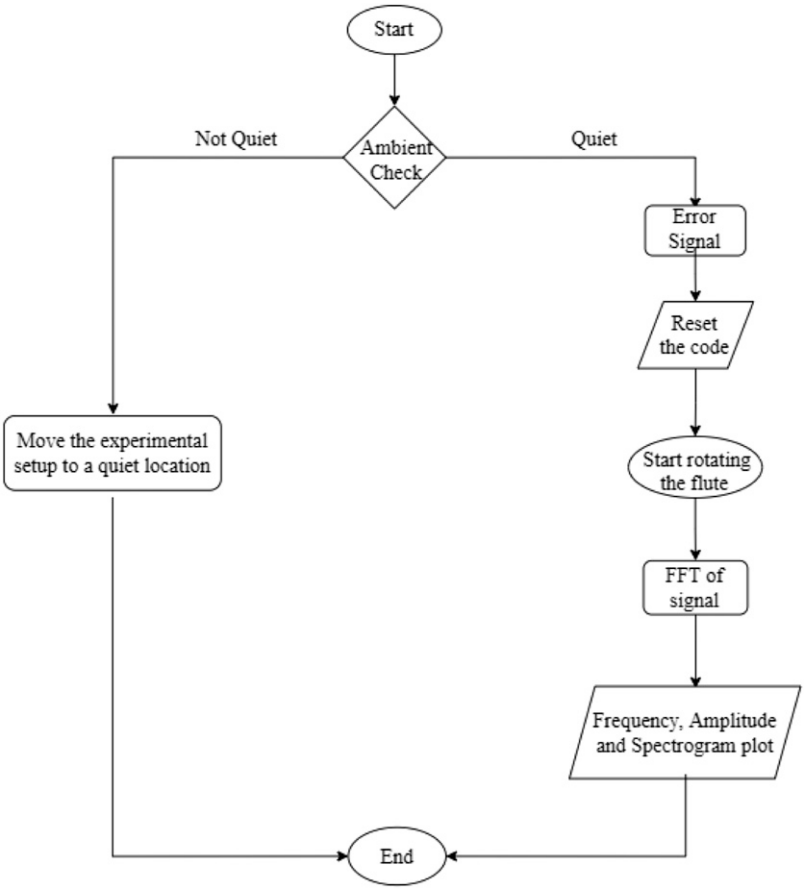

Figure 7. Experiment methodology.

three-dimensional compressible flow. Large Eddy Simulation (LES) with sub-grid model (Smagorinsky-Lilly) is used. Air is considered as an ideal fluid for the simulations. The grid independence has been carried to find the optimal mesh size. The mesh with 4,458,632 elements found to be optimal and considered for further simulation. The minimum and average size of the elements are 5.71×10^{-13} m^3 and 4.26×10^{-9} m^3 respectively. The computational geometry and boundary conditions used in the simulations are presented in Figure 8 with a 2D Y-Z plane view of the whole domain.

The following boundary conditions were incorporated in the CFD analysis:

(i) *Flute inlet:* Pressure inlet boundary condition has been adopted at the inlet to the flute. The inlet pressure has been calculated based on centrifugal force by using the equation (1) for $\omega = 11.1$ rad/sec. The pressure at the inlet to the flute is found to be 46 Pa (gauge).

$$\frac{dP}{dz} = \rho\omega^2 z \tag{1}$$

$$v = r\omega \tag{2}$$

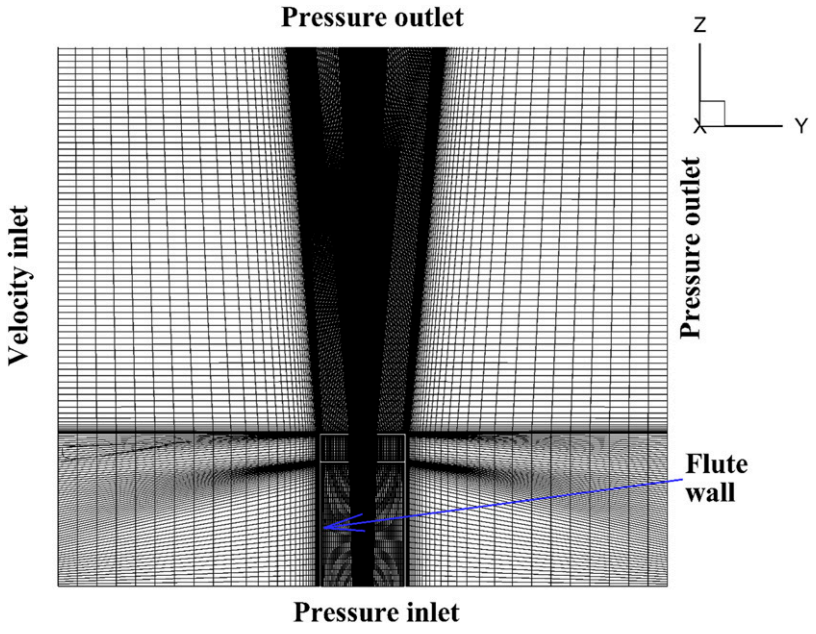

Figure 8. Schematic of mesh with boundary conditions in Y-Z plane.

$$\omega = \frac{2\pi N}{60} \tag{3}$$

(ii) *Inlet to computational domain:* Velocity inlet boundary condition has been applied at the inlet to computational domain. The velocity at the inlet has been calculated by using equation (2) for ω = 11.1 rad/sec and flute length 82 cm. The velocity at the inlet found to be 4.44 m/s Pa.
(iii) *Outlet:* The pressure outlet boundary condition is specified at the outlet plane.
(iv) *Flute wall:* no-slip boundary conditions are used for flute walls and rims.

Results and discussions

Acoustic generation by the z-axis rotation

When the flute is rotated about the z-axis at approximately 100 r/min, it can be observed that the sound generated at the upper end of the flute has a peak frequency range of 1000–1500 Hz. When the flute is imparted a rotation, it is measured that the incoming flow strikes the top part of the flute with a velocity of approximately 4.51 m/s. An intense but discontinuous range of low-level frequencies can be observed, with a much more continuous range at around 1500 Hz. The analysis is shown in Figure 9. This sound is generated because of the centrifugal motion of the air particles inside the flute, which is coupled and correlated with the concept of flow around a cylinder, with the consequent vortex-shedding mechanism and the resulting pressure fluctuations. The power spectrum of Baster flute at low frequencies is also observed in this experiment. It can be possible that

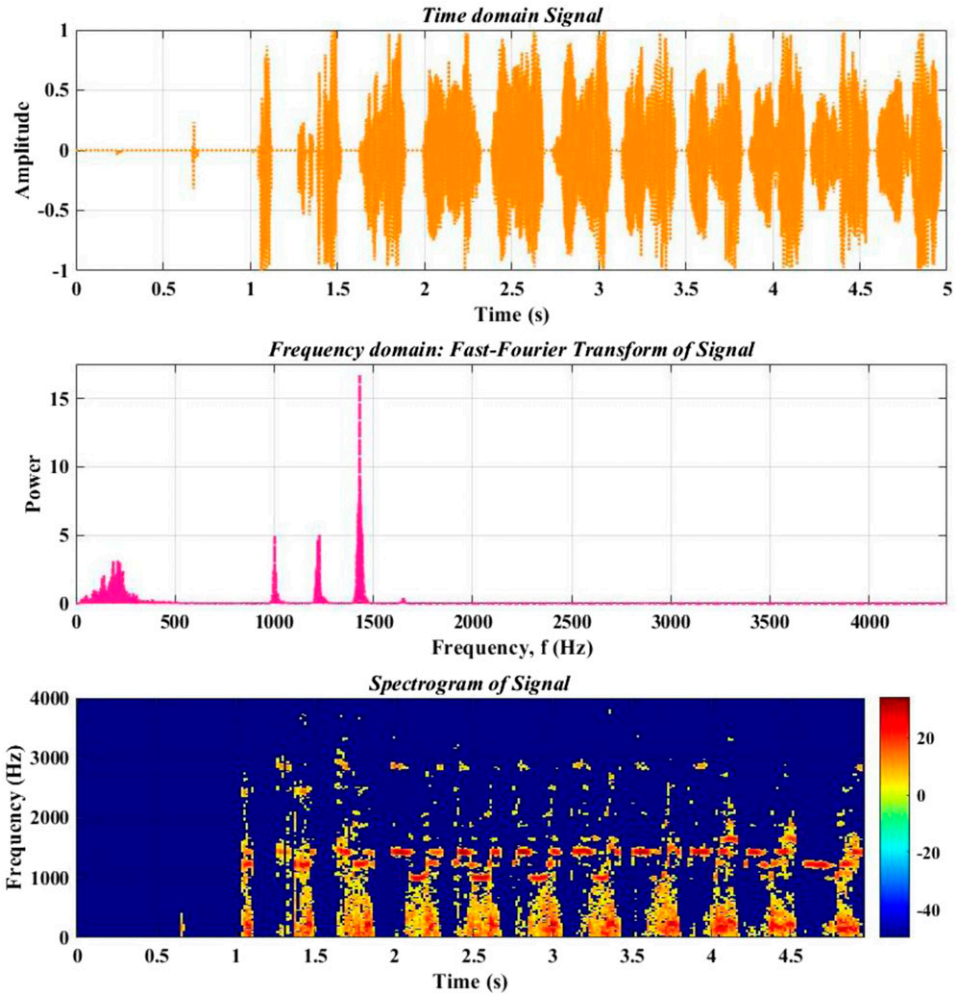

Figure 9. Experimental analysis of the flute acoustic signature when it is rotated about the z-axis.

the wave propagation between the rim, wave generation around the outer rim of flute due to its rotation could be the reason of these power distribution at low frequencies. The harmonic analysis of Baster flute is not considered in this study because it is required more precise mathematical model of Baster flute. The scope of this study is only to gain the preliminary knowledge of sound generation through Baster flute.

As shown in Figure 10, when the flute is rotated about the z-axis, the velocity of the flute's upper end is higher compared to the lower end, where the flute is pivoted. This scenario is correlated with the flow around a cylinder where stagnation points are created at the adjacent ends of the cylinder.[39] The stagnation point is a zone of high pressure and there is a point of extremely low pressure on top of the cylinder. This is a critical point where the pressure is extremely low. At the top of the cylinder, a local low-pressure gradient has developed because of the incoming high velocity of the fluid when compared to the pivoted end of the flute. Therefore, the air flows from bottom to top, moving away

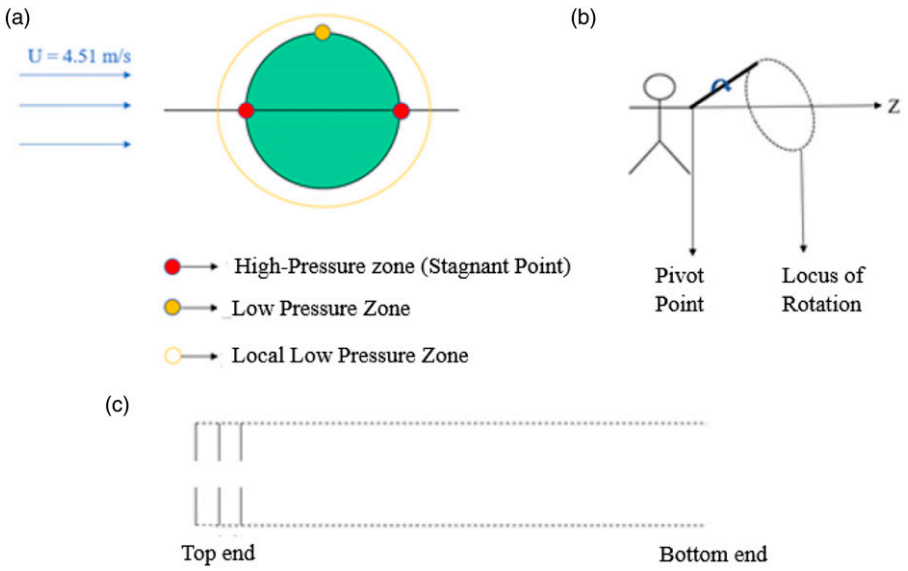

Figure 10. (a) The top part of the flute correlated with flow over a cylinder with a local low-pressure gradient, (b) Schematic of rotation about the z-axis, and (c) Schematic of the flute showing the rims present inside the flute.

from the center. The concept of airflow in the flute while rotating is shown and discussed in Figure 11.

When the flute starts rotating about its pivot point, acoustic signals are generated from pressure fluctuations, and the rims present inside the flute at the top end start acting as resonators. When the air strikes the rim, it creates pressure fluctuations, leading to disruption of flow, and the energy lost is dissipated in the form of sound. This shows the significance of obstacles in airflow for the generation of acoustics.[40]

The other factor which comes into play is the Reynolds number, which determines the flow characteristics, i.e., whether laminar or turbulent. If the Reynolds number is high for a particular flow condition, the amplitude and frequency of the generated sound will be high. In this case, if the RPM of the flute is increased, then the velocity with which the flow will strike the rims will be higher, thus leading to a greater magnitude of amplitude and frequency. Moreover, noise introduced by the rotation of the flute and the microphone itself should also be accounted for. Rotating the cylindrical flute causes pressure fluctuations due to the von Karman vortex street created in the wake, which may be audible as "noise" when combined with the complex pressure fluctuations at the microphone end of the cylindrical flute. Thus, the collected "background data," in our experiments is the sum of the "noise" from pressure changes owing to cylinder movement and other sources.

Acoustic generation along the y-axis rotation

The frequency generated in both cases of experimentation, i.e., in the z and y axes is nearly the same, which is shown in both Figures 9 and 12. The methodology of both the experiments is the same. This also indicates that the acoustics generation at the top end of the flute resonates at 1500 Hz. Again, an

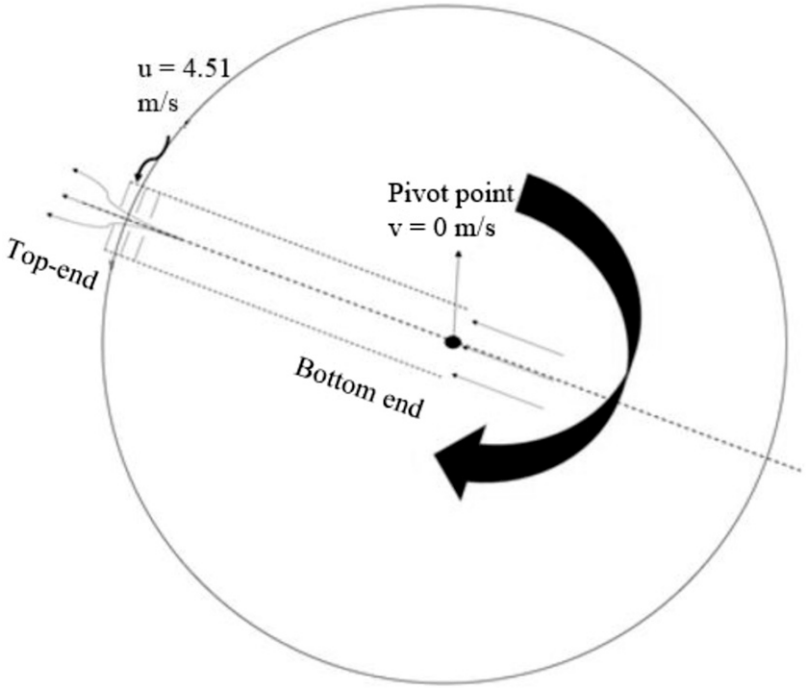

Figure 11. Direction of airflow inside the flute while rotating it.

intense but discontinuous range of low-level frequencies can be observed on the lower end of the spectrogram, with a much more continuous range at above, below, and around 1500 Hz. The significance of rims present inside the flute is to enhance the acoustic generation, and perhaps if more rims were present inside the flute, the amplitude of the sound would be much higher.

A significant observation made is that a full rotation is not necessary for the generation of acoustics; instead, if the flute is given the slightest of rotation it generates sound. This is valid for either of the axes. If the angular velocity of the flute is increased then it directly affects the frequency and amplitude of acoustics generated, i.e., the greater the angular velocity of the flute is the frequency and amplitude. The restriction of angular velocity comes when the rotation is imparted manually, especially along the y axis, since the manoeuvrability to rotate around this axis at high speed cannot be performed with ease.

Preliminary mathematical formulation

When the flute is rotated about either axis, it produces approximately the same frequency (1500 Hz). As can be seen in Figure 13, the reason behind the airflow from bottom to top is due to centrifugal force acting on the air particles inside the flute which in the rotating domain moves away from the centre. To understand the pressure difference created this is correlated with the concept of flow around a cylinder. The upper half of the flute is moving at a higher velocity as compared to the other end (pivot point). This irregularity in pressure creates variable stagnation points at both ends, which leads to the creation of a local low-pressure gradient at the top of the flute.

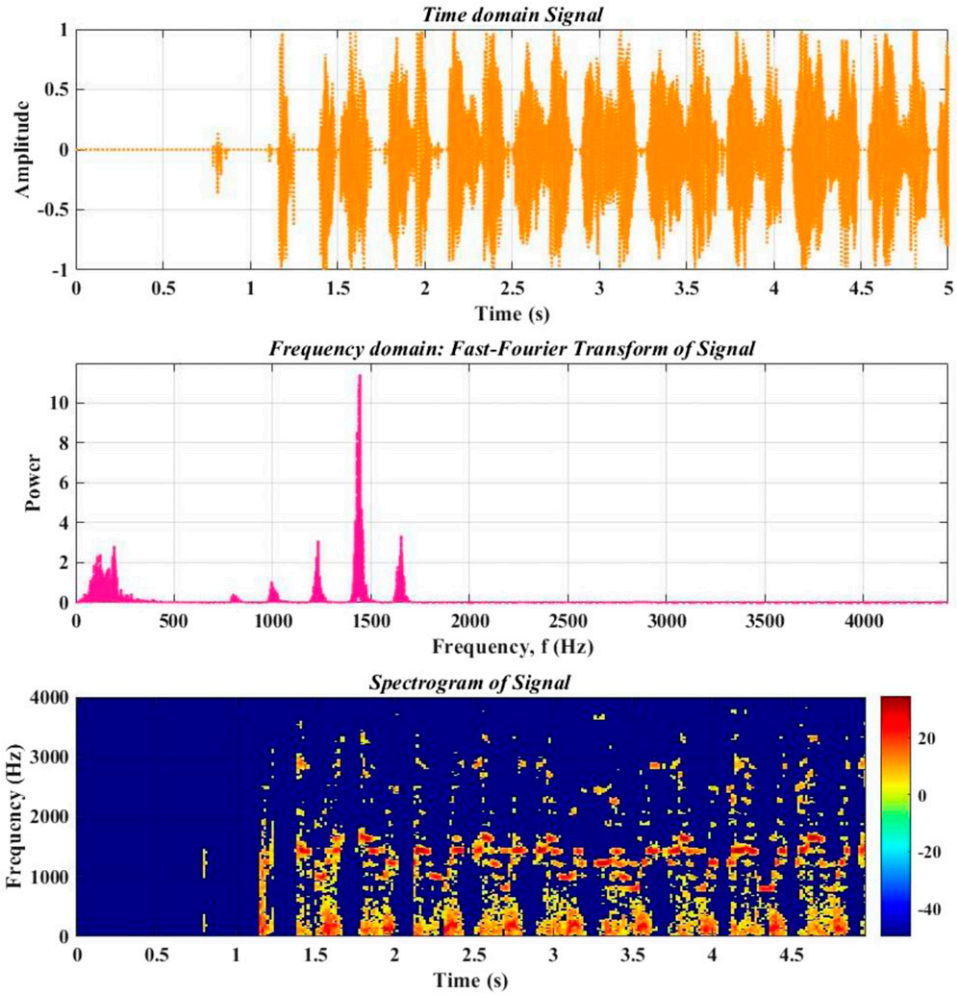

Figure 12. Experimental analysis of the flute acoustic signature when it is rotated about the y-axis.

Equations (1)–(3) are used for the calculation of the pressure difference between point 1 and point 2, the linear velocity of the flute, and angular velocity. From these calculations, the linear velocity of the flute comes out to be approximately 4.51 m/s, and the pressure near the rims is approximately 101,371 Pa. The angular velocity of the flute is approximately 100 r/min, as measured from high-speed imaging of the experiments.

The acoustic signals generated at the rim is due to the pressure difference and the flow obstruction, leading to pressure fluctuations. Apart from pressure fluctuations, these are free vortices that are shed during flow obstruction, and energy is dissipated in the form of sound. When the flute is rotated about either of the axes with the bottom end closed, it generates no sound, which implies no pressure gradients developed on both sides of the flute that could lead to airflow in the flute. Upon hitting a rim, a phenomenon called jet-tone occurs, which leads to the formation of two rows of vortices rotating in opposite directions on the two sides of the central streamline. When the jet of air tries to pass through the tiny slit, a weak but audible sound is produced. This sound produced is

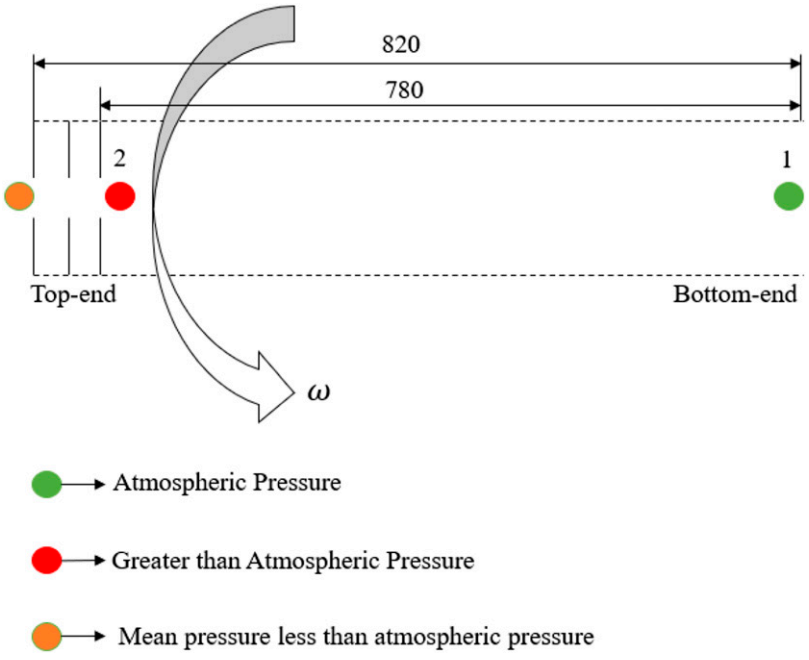

Figure 13. Pressure contours of the flute in the rotating domain.

called a Jet note.[41] The frequency of this note can be formulated as below $f = 0.045\frac{v}{a}$. Here, f denotes frequency, v is the velocity of the efflux and a is the width of the slit. Substituting the values that are experimentally obtained, $f = 1500\,Hz$, $a = 10mm = 0.01m$, we get $v = 333.33\,m/s$, which is the sound of the outgoing efflux. These calculations are done in the static domain rather than the rotating domain. Hence, the actual value of the efflux will be much lower when compared to this value. Also, large eddy simulations (LES) are done, which help to quantify the velocity of the efflux in the rotating domain.

In Figure 14 shown below, when the flute is rotated in clockwise motion, the pressure gradient goes as low as 15,000 Pa or 15 kPa near the edges, indicating the high amount of pressure generated that produces the sound. Also visible is a stagnation point, which is made as the air flowing over the flute creates drag on the efflux coming from inside the flute negating the air flow. A decrease in velocity is also observed when compared to the theoretical value of static domain, as seen in Figure 15, where it is visible that near the edges of the rims, due to large variation in pressure, the velocity only goes up to 120 m/s. Even though the actual velocity is nearly three times smaller than the theoretical velocity, a sound is nonetheless produced.

Comparison between double rim and triple rim configuration

As is evident in Figures 16 and 17, a flute with 3 rims produces a power-frequency curve with three noticeable peaks when compared with two rims, which gives us a power-frequency curve with only two peaks. It can also be observed that the power produced in the three-rim flute is higher than in the two-rim flute. The three-rim flute also generates the harmonic frequency with lower power other than resonant frequency. The power produced in three-rim flute is distributed

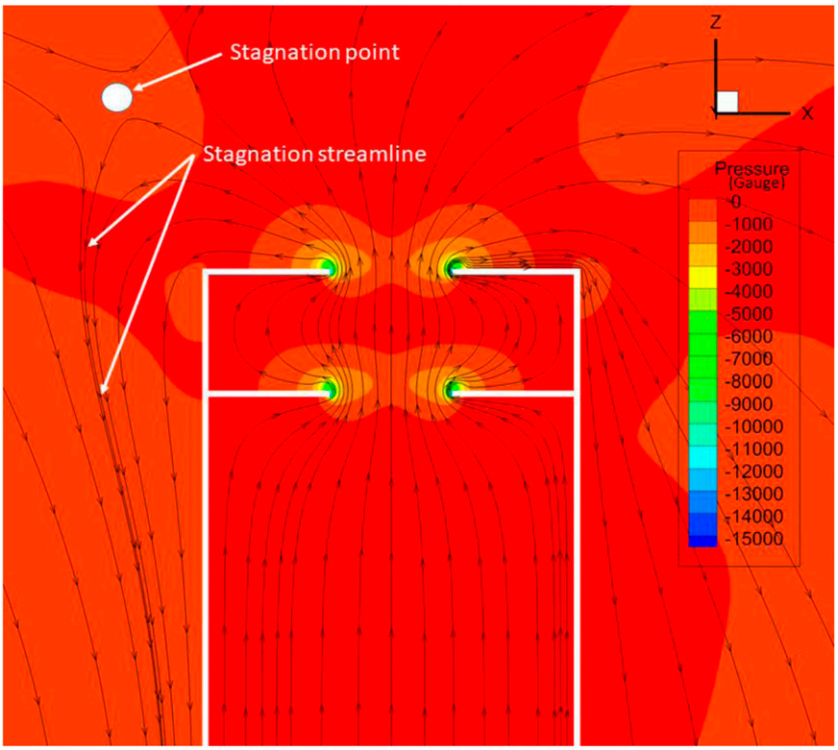

Figure 14. Large eddy simulation showing the pressure (gauge) gradient in Pascals and the flow of air while the flute rotates in clockwise motion.

in these other frequencies. It is possible that number of rims and their spacing size is one of the reasons of the power distribution in different frequency. Similarly in two-rim flute, power is distributed at harmonic frequency (other than resonant frequency 1500 Hz) with higher amplitude. The axis of rotation is also affecting the power of distribution in Baster flute with different number of rims as shown in Figures 16 and 17. About Y axis rotation, the power is distributed in lower and higher both frequency side (with respect to 1500 Hz) in three-rim and two-rim flute.

A relationship is also developed to prove these experimental observations correct theoretically, which is described below.

From Figure 18, it can be deduced that as the airflow strikes the first rim, its laminar nature turns turbulent, wherein its initial velocity (v_{in}) decreases to v_1. This stream of turbulent air then strikes the second rim, where its velocity further decreases to v_2, and then from v_2 to v_3. Edge tone also plays a role in the generation of the sound heard. The sound passes through the first slit in a laminar fashion, becomes turbulent and strikes the second rim. This second rim upon the striking of the air flow, acts as a resonator and produces sound. The second rim then acts as a slit to let this air stream through which then hits the third rim, repeating the phenomena. When exiting the third slit, only the jet tone effect takes place.

From this, it can be written, $v_1 > v_2 > v_3$,which describes the loss of velocity of the incoming air due to vortex formation in every subsequent step. To mathematically model this

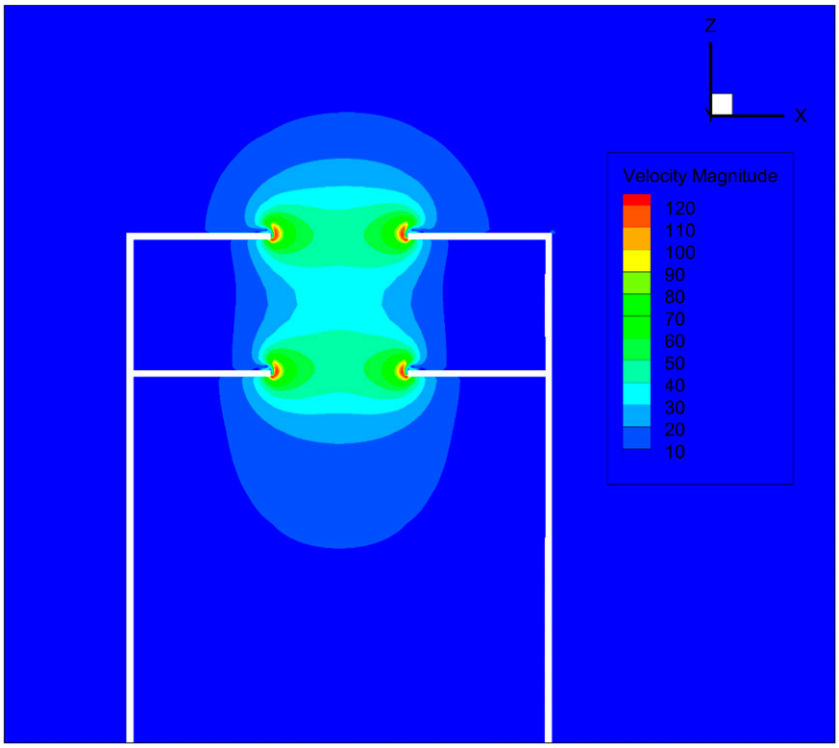

Figure 15. Large eddy simulation demonstrating the velocity magnitude as the flute rotates in clockwise motion. Note that the velocity magnitudes are in SI units, and pressures shown are gage pressures.

relationship, using the jet tone equation, it is given that the velocity of the airflow is directly proportional to the frequency of air produced, $v \propto f$ .This implies that, $f_1 > f_2 > f_3$, demonstrating that the frequency produced by each ring decreases, which also helps in describing its relationship with amplitude as amplitude is inversely proportional to frequency produced, it implies, $A_1 < A_2 < A_3$. Since energy is directly proportional to the square of the amplitude, the decrease in velocity leads to a loss of kinetic energy in the form of heat energy and sound energy. Since energy is directly proportional to the square of amplitude, $\propto A^2$. This combination of $A_1 + A_2 + A_3$ is the sound that is produced due to this energy loss. From this, it can be deduced that the more slits the flute has, the higher the amplitude of the sound, which increases

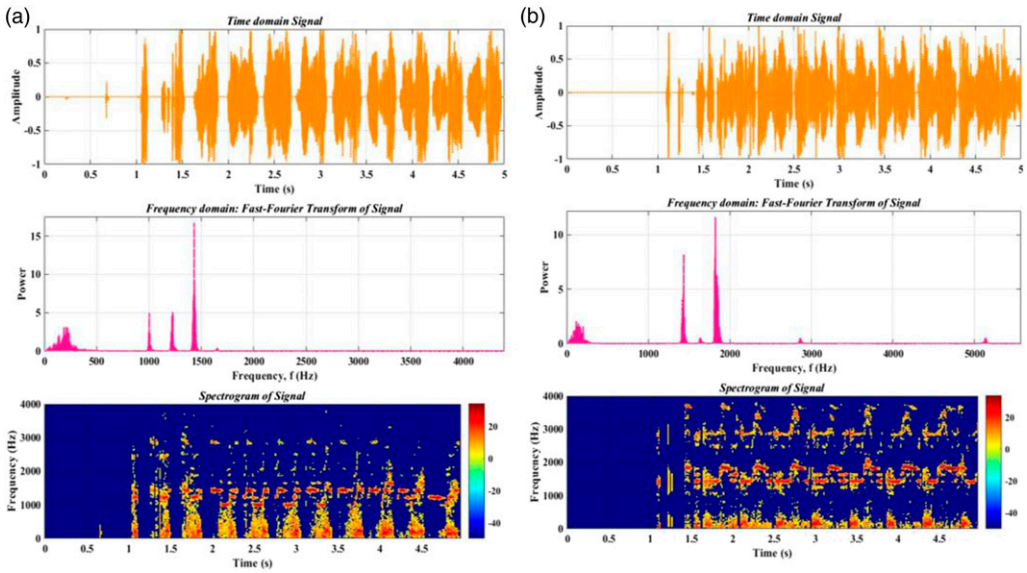

Figure 16. Comparison of (a) Experimental analysis of Flute acoustic when it is rotated about the z axis in flute with 3 rims and (b) Experimental analysis of Flute acoustic when it is rotated about the z axis in flute with 2 rims.

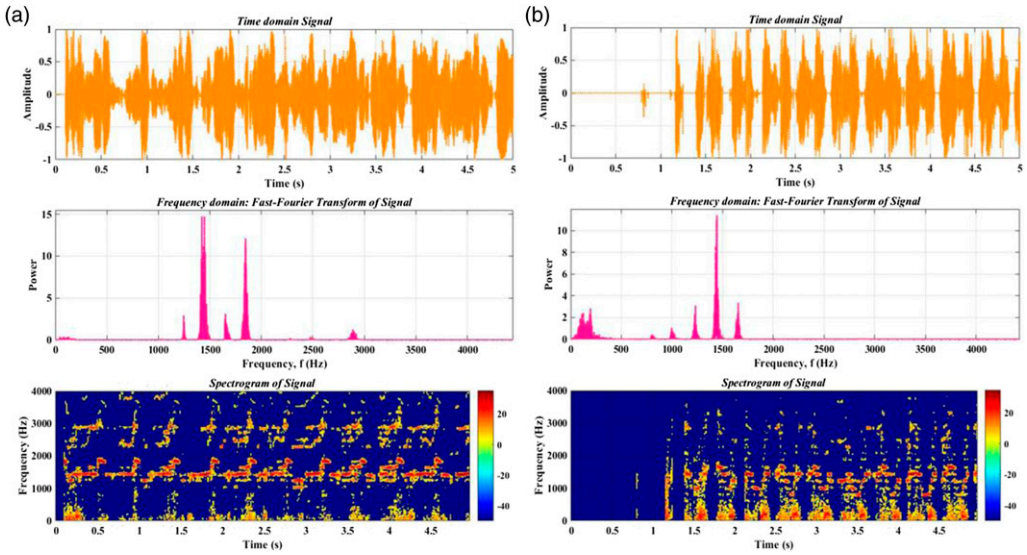

Figure 17. Comparison of (a) Experimental analysis of Flute acoustic when it is rotated about the y-axis in flute with 3 rims and (b) Experimental analysis of Flute acoustic when it is rotated about the y-axis in flute with 2 rims.

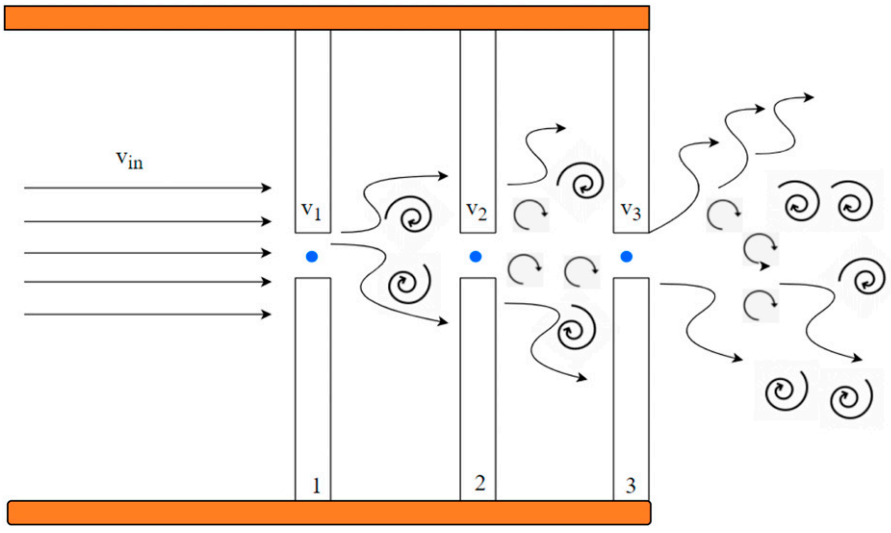

Figure 18. Change in the flow of incoming air as it strikes the rims inside the flute.

the loudness of the sound produced. However, even though only jet tone is used to quantify the relationship between the number of slits and amplitude, the theory of edge tone also plays a role in generating the sound heard.

Conclusion

The Bastar flute holds an important place in the Gond community which is one of the many tribes present in Chhattisgarh, India. They have been using this flute along with other instruments for various purposes including hunting and community festivities. The current study focuses on the characterization of sound produced by these flutes using FFT and spectrogram analysis and attempts to explain the mechanism of sound generation through analytical calculations and computational simulations. The study of these flutes are intriguing, particularly because the sound generation mechanism is a blend of jet tone and edge tone. Particularly, experiments were conducted on two-rimmed and three-rimmed Bastar flutes to specifically understand the role of rims in the sound generation.

The recorded data demonstrates the importance of rims present in the flute, where each rim produced its frequency which could be observed in experimentation. The domain used is the rotating domain, which leads to the compression of the acting fluid which is air in our case. The flutes are rotated in various axes and a variety of motions. The results recorded were analyzed and compared to a three-rimmed flute where it can be observed that a three-rimmed flute produced more and louder sound than a two-rimmed flute. In future, the researchers can observe the production of sound in domains other than the rotating domain, which could help solidify the model developed using the Jet tone phenomenon. Flow visualization techniques along with computational methods using specific models can also be employed. Finally, the specific role of each rim in producing the sound of the flute, as extricated from the noise of the Karman vortex noise produced by the flute and microphone rotation should be explored.

Acknowledgements

The authors would like to thank the University of Petroleum and Energy Studies, Dehradun for allowing us to conduct our experiments on their campus.

Declaration of conflicting interests

The author(s) declared no potential conflicts of interest with respect to the research, authorship, and/or publication of this article.

Funding

The author(s) disclosed receipt of the following financial support for the research, authorship, and/or publication of this article: This work was supported by the IKS division of All India Council for Technical Education under sanction order #**F.No: AICTE/IKS/RFP2/2021-22/18,** which motivated us to carry out this study.

ORCID iDs

Ashish Karn https://orcid.org/0000-0003-0671-4285
Ramesh Kumar Donga https://orcid.org/0000-0002-0306-1648
Naman Agarwal https://orcid.org/0000-0003-0320-0238

References

1. Hopkins WD, Taglialatela JP and Leavens DA. Chimpanzees differentially produce novel vocalizations to capture the attention of a human. *Anim Behav* 2007; 73(2): 281–286. DOI: 10.1016/J.ANBEHAV.2006.08.004
2. Jahani A, Kalantary S and Alitavoli A. An application of artificial intelligence techniques in prediction of birds soundscape impact on tourists' mental restoration in natural urban areas. *Urban For Urban Green* 2021; 61: 127088. DOI: 10.1016/J.UFUG.2021.127088
3. Rocchesso D, Delle Monache S and Barrass S. Interaction by ear. *Int J Human-Computer Stud* 2019; 131: 152–159. DOI: 10.1016/J.IJHCS.2019.05.012
4. Chris. 5 Types of musical instruments. [Online] (2021, accessed 28 December 2022).
5. Raman CV. On some Indian stringed instruments. [Online] (1921, accessed 19 April 2022).
6. Raman CV. The Indian musical drums. *Proc Indian Acad Sci - Section A* 1934; 1(3): 179–188. DOI: 10.1007/BF03035705
7. Raman CV and Kumar S. Musical drums with harmonic overtones. *Nature* 1920; 104(2620): 500. DOI: 10.1038/104500a0
8. von Hornbostel EM and Sachs C. Classification of musical instruments: translated from the original German by Anthony Baines and Klaus P. Wachsmann. *Galpin Soc J* 1961; 14: 3. DOI: 10.2307/842168
9. Karjalainen M, Backman J and Polkki J. Analysis, modeling, and real-time sound synthesis of the kantele, a traditional Finnish string instrument. *Proc - ICASSP IEEE Int Conf Acoust Speech Signal Process* 1993; 1. DOI: 10.1109/ICASSP.1993.319097
10. Siswanto WA, Che Wahab WMA, Yahya MN, et al. A platform for digital reproduction sound of traditional musical instrument Kompang. *Appl Mech Mater* 2014; 660: 823–827. DOI: 10.4028/WWW.SCIENTIFIC.NET/AMM.660.823
11. Suprapto YK, Purnama IKE, Hanadi M, et al. Sound modeling of javanese traditional music instrument. In: International Conference on Instrumentation, Communication, Information Technology, and

Biomedical Engineering 2009; ICICI-. BME 2009, Bandung, Indonesia, 23-25 November 2009. DOI: 10.1109/ICICI-BME.2009.5417254
12. Computational analysis of style in Irish traditional flute playing. http://www.open-access.bcu.ac.uk/8759/ (accessed 11 April 2022).
13. Someya S and Okamoto K. Measurement of the flow and its vibration in Japanese traditional bamboo flute using the dynamic PIV. *J Vis* 2007; 10(4): 397–404. DOI: 10.1007/BF03181898
14. Leaf H. English medieval bone flutes: a brief introduction *The Galpin Society Journal* 2006; 59: 13–19
15. Kasliwal S. Classical musical instruments. *snarepository.nvli* 2022. [Online].(accessed 18 April 2022)
16. Macdonell A and Keith A. *Vedic index of names and subjects*, 1995. https://snarepository.nvli.in.
17. Praful K and Sudarshan B. Experimental study on two-octave Indian flute acoustics. In: *Aerospace and associated technology*. Routledge, 2022, pp. 87–94.
18. Benade AH. *Fundamentals of musical acoustics*. North Chelmsford: Courier Corporation, 1990.
19. Coltman JW. Sounding mechanism of the flute and organ pipe. *J Acoust Soc Am* 1968; 44(4): 983–992.
20. Nederveen CJ. Acoustical aspects of woodwind instruments. PhD dissertations. Frits Knuf, 1969.
21. Fletcher N. Materials and musical instruments. *Acoustics Australia* 2012; 40(2).
22. Wolfe J, Smith JR, Tann J, et al. Acoustic impedance spectra of classical and modern flutes. *J Sound Vib* 2001; 243(1): 127–144.
23. Dickens PA. Flute acoustics: measurements, modelling and design. PhD dissertation. University of New South Wales, 2007.
24. Montagu J. *Origins and development of musical instruments*. [Online] (2007, accessed 19 April 2022).
25. Solvyns B. A collection of two hundred and fifty coloured etchings descriptive of the manners, customs and dresses of the Hindoos, Sec XI, No. 36, 1799.
26. Kaufmann W. The Musical Instruments of the Hill Maria, Jhoria, and Bastar Muria Gond Tribes. *Ethnomusicology* 1961; 5(1): 1–9
27. Jain SK. Wooden musical instruments of the Gonds of Central India. *Ethnomusicology* 1965; 9(1): 39. DOI: 10.2307/850416
28. Yoshikawa S, Tashiro H and Sakamoto Y. Experimental examination of vortex-sound generation in an organ pipe: a proposal of jet vortex-layer formation model. *J Sound Vib* 2012; 331(11): 2558–2577. DOI: 10.1016/j.jsv.2012.01.026
29. Nelson PA, Halliwell NA and Doak PE. Fluid dynamics of a flow excited resonance, Part I: experiment. *J Sound Vib* 1981; 78(1): 15–38.
30. Nelson PA, Halliwell NA and Doak PE. Fluid dynamics of a flow excited resonance, part ii: flow acoustic interaction, 1983.
31. Howe MS. Contributions to the theory of aerodynamic sound, with application to excess jet noise and the theory of the flute, 1975.
32. Howe MS. The dissipation of sound at an edge, 1980.
33. Salikuddin M and Ahuja KK. Acoustic power dissipation on radiation through duct terminations experiments, 1983.
34. van Oudheusden BW. PIV-based pressure measurement. *Meas Sci Technol* 2013; 24(3): 032001. DOI: 10.1088/0957-0233/24/3/032001
35. Mohamed S and Ziada S. PIV measurements of aeroacoustic sources of A shallow cavity in A pipeline. In Pressure Vessels and Piping Conference (Vol. 46018, p. V004T04A054), American Society of Mechanical Engineers, 2014.
36. Lorenzoni V, Tuinstra M and Moore P, et al. (2009) Aeroacoustic analysis of a rod-airfoil flow by means of time-resolved PIV. In In 15th AIAA/CEAS Aeroacoustics Conference (30th AIAA Aeroacoustics Conference) (p. 3298).

37. Astoul T, Wissocq G, Boussuge JF, et al. Lattice Boltzmann method for computational aeroacoustics on non-uniform meshes: a direct grid coupling approach. *J Comput Phys* 2021; 447(Dec): 110667. DOI: 10.1016/j.jcp.2021.110667
38. Guasch O, Pont A, Baiges J, et al. Finite element hybrid and direct computational aeroacoustics at low Mach numbers in slow time-dependent domains. *Comput Fluids* 2022; 239: 105394. DOI: 10.1016/j.compfluid.2022.105394
39. Sheridan J, Lin JC and Rockwell D (1997). Flow past a cylinder close to a free surface. *Journal of Fluid Mechanics*, 330, 1–30.
40. Lighthill MJ. (1997). On sound generated aerodynamically I. General theory. Proceedings of the Royal Society of London. Series A. *Mathematical and Physical Sciences*, 211(1107), 564–587.
41. Ghosh M and Bhattacharya D. *A textbook of oscillations, waves and acoustics*, 2016.

Appendix

Nomenclature

Symbol	Description
ρ	Density
z	Axis
ω	Angular velocity
r	The radius of the flute
N	Rotation per minute (RPM)
f	Frequency
v	The velocity of the incoming air stream
A	Amplitude of sound produced
a	Slit width
E	Energy of the sound wave